USING STEREO VISION AND TACTILE SENSOR FEATURES
For Grasp Planning Control

Madjid Boudaba[1], Nicolas Gorges[2], Heinz Woern[2] and Alicia Casals[3]

[1]*TES Electonic Solution GmbH, Zettachring 8, 70567 Stuttgart, Germany*

[2]*Institute of Process Control and Robotics, University of Karlsruhe*
Engle-Bunte-Ring 8-Gebaeude 40.28, 76131 Karlsruhe, Germany

[3]*GRINS: Research Group on Intelligent Robots and Systems*
Technical University of Catalonia, Pau Gargallo 5, 08028 Barcelona, Spain

Keywords: Stereo vision, Tactile sensors, Grasp planning, Features matching.

Abstract: Planning the grasp positions either from vision or tactile sensors one can expect various uncertainties. This paper describes a scheme that match visual stereo and tactile data based on stereo vision and tactile sensors. For grasp planning, initially, the grasping positions are generated from stereo features, then the feedback of tactile features is used to match these positions. The result of the matching algorithm is used to control the grasping positions. The grasping process proposed is experimented with an anthropomorphic robotic system.

1 INTRODUCTION

In recent years, considerable research in robotic grasping systems has been published. The proposed system works by using the principle of *sensing-planning-action*. To place our approach in perspective, we review existing methods for sensor based planning for grasping. The existing literature can be broadly classified into three categories; vision based, tactile based and both vision-tactile based. For all categories, the extracted image features are key factors, they can range from geometric primitives such as edges, lines, vertices and circles to optical flow estimates. The first category uses visual image features to estimate the grasping points and from them define the robot's motion with respect to the object position and orientation before performing a grasp (Yoshimi and Allen, 1994), (Maekawa et al., 1995), (Smith and Papanikolopoulos, 1996), (Sanz et al., 1998), (Kragic et al., 2001), and (Morales et al., 2002). The second category uses tactile image features to estimate the characteristics of the area in contact with the object (Berger and Khosla, 1991), (Chen et al., 1995), (Perrin et al., 2000), and (Lee and Nicholls, 2000). The last category uses data fusion from both vision and tactile sensors in order to control grasping tasks efficiently (Namiki and Ishikawa, 1999), and (Allen et al., 1999).

This paper is an extension of our previous work (Boudaba and Casals, 2006) and (Boudaba and Casals, 2007) on grasp planning using visual features. In this work, we demonstrate the utility of matching both visual and tactile image features in the context of grasping, or fingers position controlling. In our approach, we avoid using any object model, and instead, we work directly from image features to plan the grasping points. In order to avoid finger positioning errors, matching, by back projecting these tactile features into visual features is required to compute the similarity transformation that relates the grasping region with the sensitive touching area. To achieve a high level of grasping position matching efficiency, two matching schemes are considered in this paper. The first establishes grasp points correspondences between the left and right images of the stereo head. In this scheme, only the grasp positions are back projected into one side of the stereo image. A second scheme is a region matching where the whole sensitive touching area with the object is used in the back projection into the visual image. All the points belonging to the sensitive area of a tactile sensor are back-projected into the grasp region of visual features. The processing in each match is completely independent and can be performed at its own rate. Our approach based on features matching can play the

critical role of forcing the fingertips to move towards the desired positions before the grasping is executed.

2 GRASPING SYSTEM DESCRIPTION

In robotic grasping tasks, when data from several sensors are available simultaneously, it is generally necessary to precisely analyze all of them along the entire grasping process (see Figure 1). The object being extracted from a video sequence requires encoding its contour individually in a layered manner and provide at the receiver's side some enhanced visual information. In the same way, from the data being extracted from a tactile sensor, the tactile layer processes and provides the tactile information at its receiver's side. The architecture of the whole grasping system is organized into several modules, which are embedded in a distributed MCA2 (Modular Controller Architecture Version 2) software framework (Scholl et al., 2001). There are mainly three modules involved in this development; the stereo vision, tactile sensors, and grasp planning. In MCA2, every module is structured in a data vector that allows the module to receive and send the data from/to other modules, or to take any part of an output data and permute and copy it to other modules. In order to control its current functionality, every module has fully or partially access to the input data of the other modules depending on the tasks involved. For instance, the grasp planning module has full access to the input data of the sensory system and has partially access to the robot hand. Because the architecture of the system has a global planning to access to all the data available to the system, the grasp planning module can locally plan the grasping positions without having a global view of the robot's environment. For instance, the robot hand needs some information supplied by the global planning module such as grasp configurations for the object to be grasped.

2.1 Visual Layer: Feature Extraction

We consider visual features extraction in the context of a stereo head (see Figure 2). First, however, we recall the epipolar geometry technique which is motivated by considering the search of corresponding points in the stereo image pair. Since we are dealing with a stereo head, we need to extract features well suited for determining the grasp points on the first image either from the left or right side of a stereo
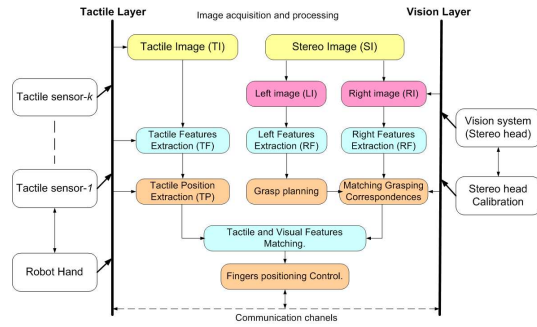

Figure 1: Grasping system description.

pair and then computing their correspondences in the second image. Given the estimated object pose, placed on the table, the full observability of the object is then projected into the left and right image planes. The visual layer takes these images and calibration data as input (see Figure 1) and provides as output a set of visual features. Segmentation is used to separate the object from the background and other objects in the environment by determining the coordinates of a closed rectangular bounding box. After segmenting the region corresponding to the object, features belonging to the object contour are extracted. A function is then constructed for parameters regrouping object features together.
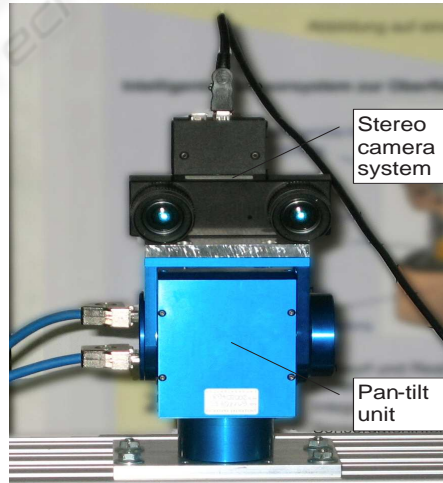

Figure 2: Stereo camera system and a Pan-tilt unit.

We denote by V a function regrouping visual parameters that is defined by

$$V = \{glist, g_{param}, com\} \qquad (1)$$

where $glist$, g_{param} and com are the visual features. During image processing, V is maintained as a doubly linked list of grasping region and intervening their

parameters as $g_1 g_{param_1}, \cdots, g_m g_{param_m}$. A grasping region g_i is defined by its ending points g_{ui} and g_{vi+1}, and its orientation ϕ with respect to the object's center of mass *com*. The resulting parameters of V fully describe the two-dimensional location of features with respect to the image plane The visual features obtained can be used as input data for both, grasp planning and grasp position matching. For more details about this topic, we refer the reader to our previous work (Boudaba and Casals, 2007).

2.2 Tactile Layer: Feature Extraction

Unlike vision which provides global features of the object, tactile sensor provides local features when the fingertip is in contact with the object. The tactile layer shown in Figure 1 takes as input the data extracted from a set of tactile sensor (or so called **G**roup **O**f **T**actile sensor (**GOT**)) and the configuration of the robot hand and provides as output a set of tactile features. To simplify the problem, tactile features are treated as visual features using the basic results from different approaches. For the purpose of sensor features matching, extracting edge features are of interest and will be discussed in section 4. Figure 3 illustrates the PCB tactile sensor module with its memory and data control units. The sensor module (from Weiss Robotics, (K.Weiss and Woern, 2005)) consists of a sensitive area organized in matrix of 4x7 sensor cells with a spacial resolution of 3.8 mm. By using four modules, (two in each gripper finger), the parallel gripper shown in Figure 3 is equipped with a total number of 112 sensor cells.
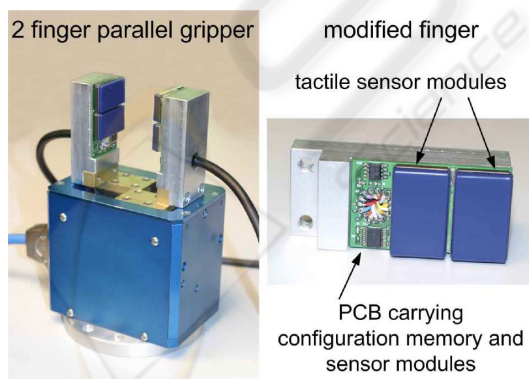

Figure 3: Gripper equipped with tactile sensor modules.

The data of the tactile sensor matrix corresponds to a two-dimensional planar image. We analyze this image using moments up to the 2nd order (Hu, 1962). The two-dimensional $(p+q)^{th}$ order moment $m_{p,q}$ of an image is defined as the following double sum over all image pixels (x,y) and their values $f(x,y)$:

$$m_{pq} = \sum_x \sum_y f(x,y) x^p y^p \qquad p,q \geq 0 \ . \quad (2)$$

The moment $m_{0,0}$ constitutes the resulting force exerted on the sensor. The center of gravity $\underline{cog} = (x_c, y_c)^T$ of this force can be computed as follows:

$$x_c = \frac{m_{10}}{m_{00}}, \quad y_c = \frac{m_{01}}{m_{00}} \ . \quad (3)$$

The center of gravity of each tactile sensor matrix determines a contact point of the gripper.

3 GRASP POSITION MATCHING

The Grasping system can be explained in more detail through a set of tasks. In order to complete the grasp matching process, it is necessary to find the relationship between their Cartesian coordinate frames (see Figure 4).
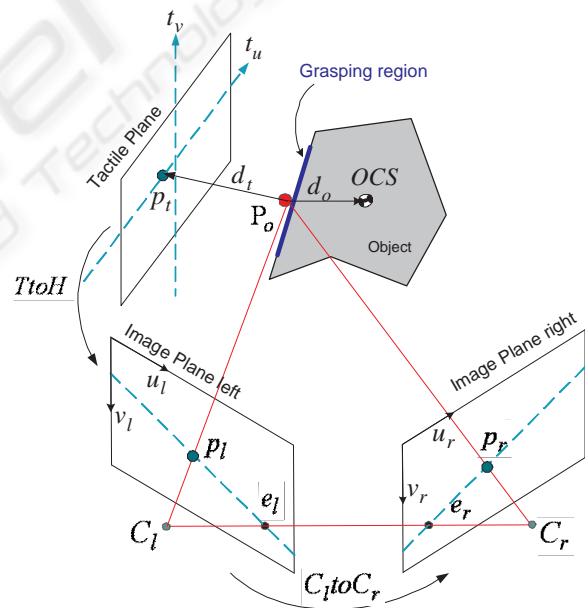

Figure 4: Sensor frames relationship for grasping.

We define these frames as follows:

- **HCS.** Head Coordinate System has a stand alone configuration of stereo head. The fixation of the head is assured by controlling the pan-tilt angle. The offset to the object coordinate system (**OCS**) is constant.

- **GCS.** Gripper Coordinate System (also known as the end effector frame) is determinated by controlling the angular configuration of the robot arm. The robot arm moves over itself and the measurements given by all joints enable the system to determine the Tool-Center-Point (TCP) relative to the robot coordinate system.

- **OCS.** Object Coordinate System is fixed on the table and does not change its position and orientation during calibration. Once the object pose relative to the stereo head (**HCS**) is determinated, the **GCS** relative to the object pose is determinated by using *robot hand - stereo head* calibration.

- **TCS.** Tactile Coordinate System. The location of **TCS** is terminated by controlling the **GCS** configuration.

- **WCS.** World Coordinate System. The location of the object position and orientation **OCS**, **HCS** and the robot base station are determinated relative to the **WCS**.

In the remaining of this work, the kinematics of the robot arm and robot hand are ignored. So far, for grasping using features matching, we have established two mapping relationships between feature frames. The first mapping implies finding the grasp points correspondence between left and right image of the stereo head ($\mathbf{C}_l to \mathbf{C}_r$). The second mapping implies matching the two apparent features into the tactile and stereo frames ($\mathbf{T} to \mathbf{H}$).

3.1 Stereo Images Matching: $\mathbf{C}_l to \mathbf{C}_r$

We adopt some notations similar, but not identical to the work of (Hartley and Zisserman, 2000) on multiple view geometry (see Figure 4). Considering a point P_o in contact with the object, its distance to the center of mass, d_o is measured and its projection into the stereo head and tactile frames is given by (p_l, p_r) and p_t, respectively. The subscripts, o, c, l, r, and t are referred to object, contact point, left and right frames, and tactile frame, respectively.

Let $p_r = (u_r, v_r, 1)^T$ and $p_l = (u_l, v_l, 1)^T$ denote the projection of P_o on the right and left images, respectively. The epipolar plane defined by the three points P_o, C_l and C_r intersects the two image planes in two epipolar lines ep_r and ep_l. The line connecting the two centers of projection $[C_l, C_r]$ intersects the image planes at the conjugate points e_r and e_l which are called epipoles. Using the projective coordinates, the epipolar constraints can be written:

$$p_l^T \mathbf{F} p_r = 0 \qquad (4)$$

where **F** is the so-called fundamental matrix which consists of a 3x3 unknown entries and can be expressed as follows:

$$\mathbf{F} = \begin{bmatrix} f_{11} & f_{12} & f_{13} \\ f_{21} & f_{22} & f_{23} \\ f_{31} & f_{32} & f_{33} \end{bmatrix} \qquad (5)$$

In the calibrated environment, the 9 unknown entries of **F** can be captured in an algebraic representation as defined by

$$\mathbf{F} = \mathbf{C}_r^{-T} \mathbf{E} \mathbf{C}_l^{-1} \qquad (6)$$

where the fundamental matrix **F** encapsulates both the intrinsic and the extrinsic parameters of the stereo head, while the essential matrix $\mathbf{E} = [\mathbf{T}]_\times \mathbf{R}$ which compactly encodes the extrinsic parameters of the stereo head can be composed of the baseline vector $\mathbf{t} = [C_r - Cl] = (t_x, 0, t_z)^T$ and the angular rotation β about the y-axis that renders the left image parallel to the right one, then we have:

$$\mathbf{E} = \begin{bmatrix} 0 & -t_z & 0 \\ t_z & 0 & -t_x \\ 0 & t_x & 0 \end{bmatrix} \begin{bmatrix} \cos(\beta) & 0 & -\sin(\beta) \\ 0 & 1 & 0 \\ \sin(\beta) & 0 & \cos(\beta) \end{bmatrix} \qquad (7)$$

$\mathbf{C}_l$ and $\mathbf{C}_r$ are the intrinsic parameter matrices of the left and right cameras defined by

$$\mathbf{C}_l = \begin{bmatrix} f_{u_l} & 0 & C_{ul} \\ 0 & f_{v_l} & C_{vl} \\ 0 & 0 & 1 \end{bmatrix}, \mathbf{C}_r = \begin{bmatrix} f_{u_r} & 0 & C_{ur} \\ 0 & f_{v_r} & C_{vr} \\ 0 & 0 & 1 \end{bmatrix} \qquad (8)$$

where u_{0l} and v_{0l} (resp. u_{0r} and v_{0r}) are the coordinates of the principle point (in pixels) of the left (resp. right) camera. (f_x, f_y) are the focal length in x and y direction.

For more details about camera calibration and related topics, we refer to the work of (Faugeras and Toscani, 1986) and (Tsai and Lenz, 1989).

3.2 Tactile and Stereo Matching: $\mathbf{T} to \mathbf{H}$

By dealing with the contact constraint, the minimum distance between a fingertip (tactile) and the object can be expressed by a parameter d_t. So keeping a fingertip in touch with the object, the condition $d_t = 0$ must be maintained, and tactile features are extracted and measured into the tactile frames. Matching these tactile features with visual features implies the computation of a similarity transformation relating the

grasping region to actual sensitive touching area. Tactile and visual features are then related by the following transformation

$$s_i = \mathbf{T}to\mathbf{H}v_i \qquad (9)$$

where s_i and v_i are points on the tactile and visual image features, respectively. $\mathbf{T}to\mathbf{H}$ is the similarity transformation given by

$$\mathbf{T}to\mathbf{H} = \begin{bmatrix} s\cos\alpha & -\sin\alpha & t_x \\ \sin\alpha & s\cos\alpha & t_y \\ 0 & 0 & 1 \end{bmatrix} \qquad (10)$$

where s, α, and $[t_x, t_y, 1]$ are scaling, rotation angle and translation vector of the tactile image with respect to the visual image, respectively.

In the calibration cases, the parameters of (10) can be computed directly using homogeneous transformation matrices between frames as shown in Figure 4.

4 IMPLEMENTATION

The implementation of our algorithm for grasping position matching using stereo vision and tactile sensor can be divided into two parts. First is related to the grasp planning using stereo vision. The second part of this implementation is related features matching between stereo vision and tactile sensor.

4.1 Grasp Planning using a Stereo Head

As stated before, the first implementation consists of computing the grasp points correspondence in the stereo vision. More formally, let $G = \{G_{v_1}, G_{v_2}, \cdots, G_{v_k}\}$ be a set of valid grasps and $G^l_{v_i} = (g^l_{\mathbf{u}_i}, g^l_{\mathbf{v}_i}, 1)^T$ be its $ith-$ determinated grasp point on the left image, next step is to compute its correspondence on the right image, $G^r_{v_i} = (g^r_{\mathbf{u}_i}, g^r_{\mathbf{v}_i}, 1)^T$. To do this, we first need to establish a mapping relationship between a line and point by exploiting the epipolar constraint defined by (4).

Let

$$L_{r_i} = \mathbf{F}G^l_{v_i}, \qquad L_{l_i} = \mathbf{F}^T G^r_{v_i} \qquad (11)$$

be the mapping equations where $\mathbf{F}^T$ is the transpose of $\mathbf{F}$ and $i := 1, 2, ..., k$ is the number of grasping points. $G^l_{v_i}$ (resp. $G^r_{v_i}$) is the determinated grasp point

on the left (resp. right) image and L_{r_i} (resp. L_{l_i}) is its corresponding epipolar line on the right (resp. left) image. By exploiting the epipolar constraint (4), the grasping points are constrained to lie along the epipolar lines L_{r_i} and L_{l_i}, respectively.

If both grasping points satisfy the relation $G^l_{v_i}\mathbf{F}G^r_{v_i} = 0$ then the lines defined by these points are coplanar. This is a necessary condition for the grasp points to correspond.

Given the parameters of a line and a grasp point in one image, the maximum deviation of a point from the line can be computed as follows:

$$d^2_{l_i} = norm(L_{l_i}, G^l_{v_i}), \quad d^2_{r_i} = norm(L_{r_i}, G^r_{v_i}) \quad (12)$$

where $d^2_{l_i}$ (resp. $d^2_{r_i}$) is the maximum deviation of a grasp point on the left (resp. right) image.

We can estimate a cost function with respect to a parameter t as follows:

$$\mathbf{C}(t) = d^2_{l_i} + d^2_{r_i} \qquad (13)$$

The minimum threshold (t_{min}) corresponds to the t_i where the cost function is minimum.

4.2 Features Matching

The second implementation consists of computing the similarity between the stereo and the tactile images features. To compare image features, the Hausdorff metric based on static features matching is used (Huttenlocher et al., 1993).

Given two feature sets: $\mathbf{S} = \{s_1, s_2, ..., s_q\}$ and $\mathbf{V} = \{v_1, v_2, ..., v_q\}$, the Hausdorff distance from the point set $\mathbf{S}$ to point set $\mathbf{V}$ is defined as

$$h(\mathbf{S}, \mathbf{V}) = maxmin_{s\in\mathbf{S}v\in\mathbf{V}} \left\| s_i - v_j \right\| \qquad (14)$$

where $\left\| s_i - v_j \right\|$ corresponds to the sum of the pixel difference and indices i and j correspond to the size of a searching window.

The matching process is evaluated according to the output of the function (14). The matching that results in the lowest cost is the one that matches the closest grasp planning. Since we want to guide the gripper toward the grasping points previously generated by the grasp planning, the solution consists of reducing the cost function (or so called grasp error) by

Table 1: Parameters measure of grasping positions and cost function: obj1, obj2.

Threshold: $t = 2$ corresponds to the maximum deviation.							
Object	Left grasp	(x_l, y_l)	d_l	Right grasp	(x_r, y_r)	d_r	**C**
obj1	$G_{v_1}^l$	358.500 365.500	2.934	$G_{v_1}^r$	313.500 377.000	2.940	17.252
	$G_{v_2}^l$	359.000 400.000	5.008	$G_{v_1}^r$	312.500 411.500	5.018	50.261
obj2	$G_{v_1}^l$	355.000 226.000	1.726	$G_{v_1}^r$	299.500 237.500	1.731	5.9768
	$G_{v_2}^l$	363.000 314.500	0.922	$G_{v_1}^r$	309.000 323.500	0.926	1.7028
	$G_{v_3}^l$	309.500 316.500	5.251	$G_{v_1}^r$	255.000 321.500	5.259	55.234

(a) **obj1:** Left image   (b) **obj1:** Right image   (c) **obj2:** Left image   (d) **obj2:** Right image

(e) Left image features   (f) Right image features   (g) Left image features   (h) Right image features
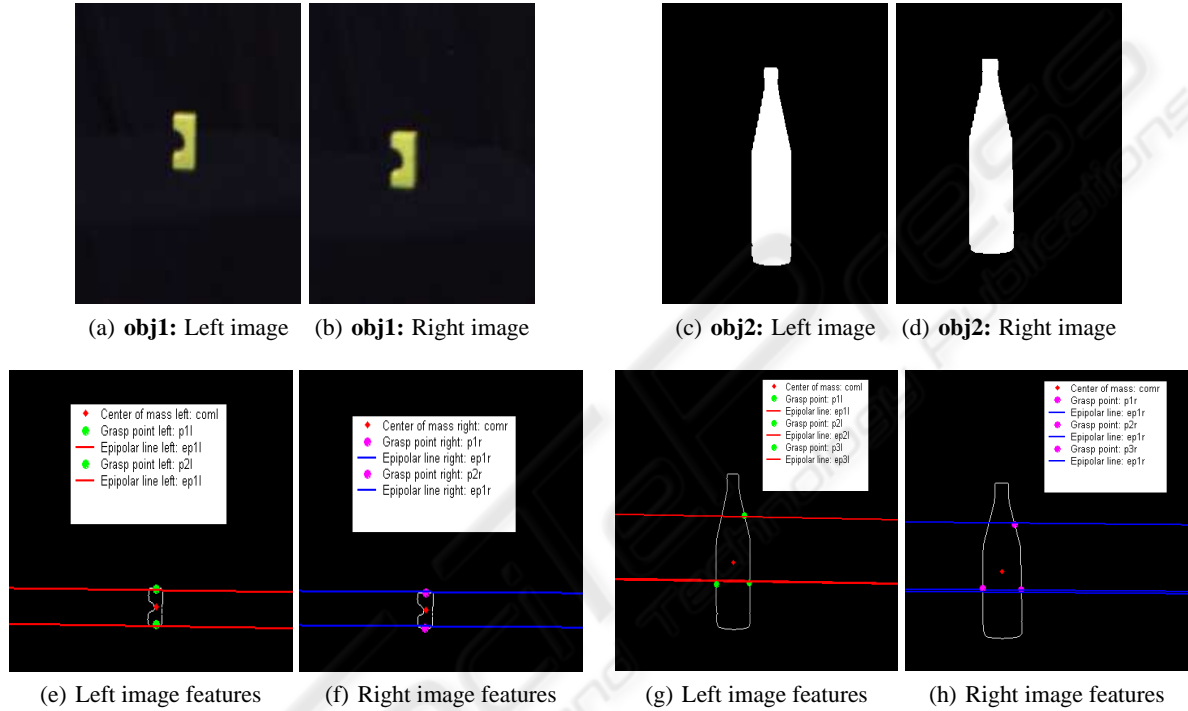
Figure 5: Result of two and three-fingered grasp planning algorithms using stereo images.

moving the tactile sensors toward these points. The cost of a solution is expressed as the total sum of contact displacements over the surface of the object from an initial contact configuration. If the result of matching is outside a given margin, then the grasp controller should launch a new measurement via joint angle and position sensors.

4.3 Matching Algorithm

- **Input:** images: im_1, im_2. features: V_1, V_2. Number of fingers: k. Fundamental matrix: **F**. Threshold t. Size of window: 7x7 pixel.
- **Output:** Grasping points: $(G_{v_i}^l, G_{v_i}^r)$, with $i := 1,...,k$. Matching: $h(\mathbf{S}, \mathbf{V})$

  ■ **Process:**

1. *Perform the features extraction tasks*

- *for $i := 1$ to 2 do*
- *extract features: $V_i := im_i$.*

2. *Perform the grasp planning tasks*

- *select V_1 on which the grasp will be performed.*
- *Get valid grasps point G_v from (1)*

3. *Perform the grasping point correspondences*

- *select V_2 on which the grasping correspondences will be performed*
- *for $i := 1$ to k do*
- *Compute $G_{v_i}^l := G_{v_i}$*
- *Compute L_{r_i} and $G_{v_i}^r$ using (11)*

4. *Perform the matching function*

- *for $i, j := 1$ to $7,7$ do*
- *Compute $h(\mathbf{S}, \mathbf{V}) \leq r$ and $h(\mathbf{S}, \mathbf{V}) \geq r$*
- *Compute pixel difference $h(\mathbf{S}, \mathbf{V})$ from (14)*

219

(a) Tactile sensor feedback: top gripper

(b) Tactile sensor feedback: bottom gripper

(c) Gripper grasping an object
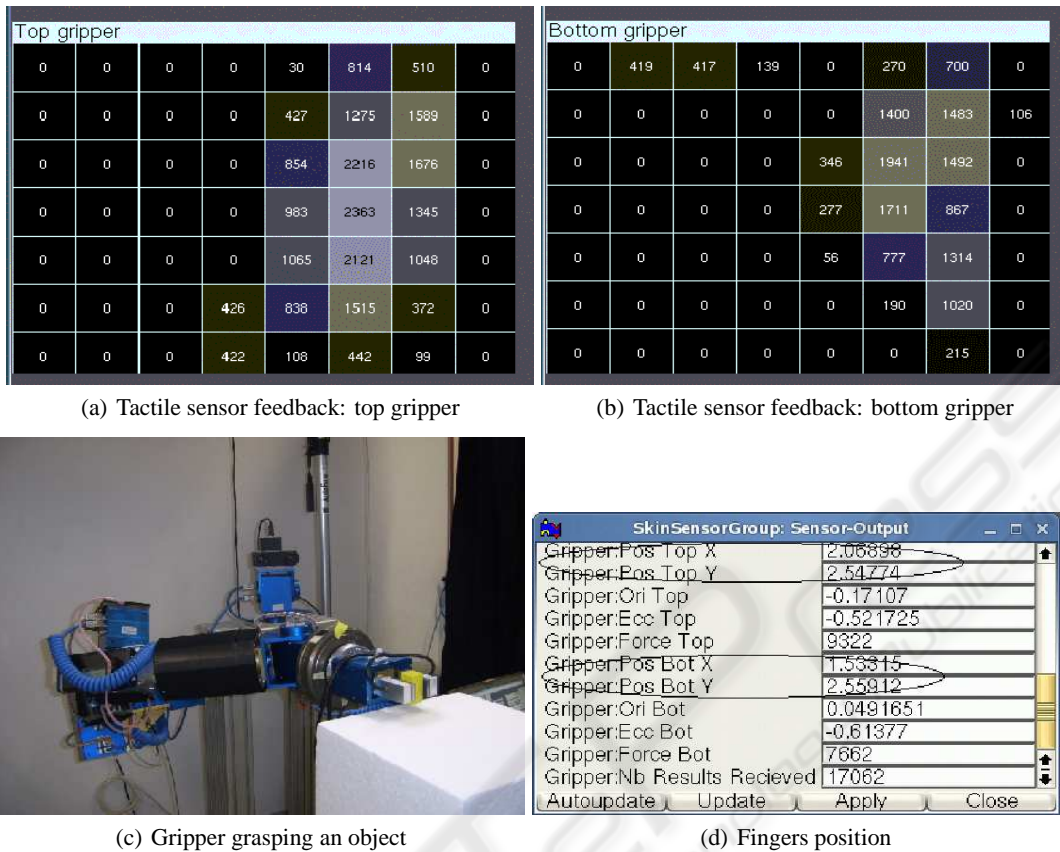

(d) Fingers position

Figure 6: The Experiment setup. (a)-(b) Tactile sensor feedback giving the sensitive area in contact with the object. (c) Object grasped with two fingers parallel gripper. (d) Tactile sensor output giving the top/bottom position of the gripper.

5. *Perform the cost function*

- *Compute $d_{l_i}^2$ and $d_{r_i}^2$ using (12)*
- *Compute $\mathbf{C}(t)$ with (13)*

6. **End.**

4.4 Experimental Results

The algorithm was implemented on our experimental system, which consists of a 7 DOF manipulator arm, a robot hand with two fingers, each one equipped with a tactile sensor module mounted directly to the finger tip, and a vision system (see Figure 6). This first prototype of anthropomorphic robot system developed by the German Research Foundation (see (Boudaba et al., 2005)) is used as platform and demonstrator for a coming generation of service robots. The grasping configuration is based on a stand-alone stereo head (MEGA-D from Videre Design) mounted on a pan-tilt controller unit equipped with a pair of 4.8 mm lenses and a fixed baseline of about 9cm. We have experimented our approach with two different kind of objects placed on a fixed table with a fixed position

and orientation (static object). Figure 5 illustrates the results obtained from our matching algorithm using stereo vision. The performance of our results (see Table 1) is validated according to a cost function $\mathbf{C}$ defined in the stereo images as the errors between grasping points. The cost that results in the lower value is the one that matches the closest grasp planning. Figures 6(b)-(d) illustrate the feedback of tactile sensor giving the top/bottom position of fingers with respect to the tactile image plane in (b) while (c)-(d) showing the top/bottom sensitive area in touch with the object.

5 CONCLUSIONS

The implementation of our algorithms for grasping points matching using stereo vision and tactile sensor have been detailed. Two schemes for grasping points matching have been included in this work. In the first scheme, stereo vision matching was used to find the grasp points correspondence between left and right images. It is shown that the quality of matching

depends strongly on the precise computation of the intrinsic and extrinsic parameters of the stereo head calibration. The performance of our results is evaluated according to a cost function defined in the stereo images as the errors between a pair of grasping points. In the second scheme, the tactile sensor provides the sensitive area of a fingertip in contact with an object which was used with the grasp region to compute the similarity between both features. Using these two matching schemes, we were able to fuse the visual grasp region with the tactile features and capabilities of reducing or avoiding the grasp positioning errors (or so called controlling the grasp planning) before executing a grasps.

REFERENCES

Allen, P., Miller, A., Oh, P., and Leibowitz, B. (1999). Integration vision, force and tactile sensing for grasping. *Int. Journal of Intell. Mechatronics*, 4(1):129–149.

Berger, A. D. and Khosla, P. K. (1991). Using tactile data for real-time feedback. *International Journal of of Robotics Research (IJR'91)*, 2(10):88–102.

Boudaba, M. and Casals, A. (2006). Grasping of planar obbjects using visual perception. In *Proc. IEEE 6th International Conference on Humanoid Robots (HUMANOIDS'06)*, pages 605–611, Genova, Italy.

Boudaba, M. and Casals, A. (2007). Grasp configuration matching using tactile and visual information. In *Proc. IEEE 4th International Conference on Informatics in Control, Automation and Robotics (ICINCO'07)*, volume Vol. II, pages 121–127, Angers, France.

Boudaba, M., Casals, A., Osswald, D., and Woern, H. (2005). Vision-based grasping point determination on objects grasping by multifingered hands. In *Proc. IEEE 6th International Conference on Field and Service Robotics*, pages 261–272, Australia.

Chen, N., Rink, R. E., and Zhang, H. (1995). Edge tracking using tactile servo. In *Proc. IEEE/RSJ International Conference on Intelligent Robots and Systems*, pages 84–99.

Faugeras, O. D. and Toscani, G. (1986). The calibration problem for stereo. In *In Proc. IEEE Conference on Computer Vision and Pattern Recognition, CVPR'86*, pages 15–20, Miami Beach, FL, USA.

Hartley, R. and Zisserman, A. (2000). *Multiple View Geometry in Computer Vision*. Cambridge University Press, England, UK.

Hu, M.-K. (1962). Visual Pattern Recognition by Moment Invariants. *IEEE Transactions on Information Theory*, 8(2):179–187.

Huttenlocher, D., Klanderman, D., and Rucklige, A. (1993). Comparing images using the hausdorff distance. *IEEE Transaction on Pattern Analysis and Machine Intelligence*, 15(9):850–863.

Kragic, D., Miller, A., and Allen, P. (2001). Real-time tracking meets online grasp planning. In *Proc. IEEE International Conference on Robotics and Automation (ICRA'2001)*, pages 2460–2465, Seoul, Korea.

K.Weiss and Woern, H. (2005). The working principle of resistive tactile sensor cells. In *Proceedings of the IEEE Int. Conf. on Mechatronics and Automation*, pages 471–476, Ontario, Canada.

Lee, M. H. and Nicholls, H. R. (2000). Tactile sensing for mechatronics - a state of the art servey. *Mechatronics*, 9:1–31.

Maekawa, H., Tanie, K., and Komoriya, K. (1995). Tactile sensor based manipulation of an unknown object by a multifingered hand with rolling contact. In *Proc. IEEE International Conference on Robotics and Automatation*, pages 743–750.

Morales, A., Sanz, P., and del Pobil, A. (2002). Heuristic vision-based computation of three-finger grasps on unknown planar objects. In *Proceedings of the IEEE/RST Int. Conf. on Intelligent Robots and Systems*, pages 1693–1698, Lausanne, Switzerland.

Namiki, A. and Ishikawa, M. (1999). Optimal grasping using visual and tactile feedback. In *Proceedings of the IEEE/RST Int. Conf. on Intelligent Robots and Systems*, pages 589–596.

Perrin, D., Smith, C., Masoud, O., and Papanikolopoulos, N. (2000). Unknown object grasping using pressure models. In *Proceedings of the IEEE International Conference on Multisensor Fusion and Integration for Intelligent Systems*, pages 575–582.

Sanz, P., del Pobil, A., Iesta, J., and Recatal, G. (1998). Vision- guided grasping of unknown objects for service robots. In *ICRA'98*, page 30183025, Leuven, Belgium.

Scholl, K. U., Albiez, J., and Gassmann, B. (2001). MCA - An Expandable Modular Controller Architecture. *3rd Real-Time Linux Workshop*.

Smith, C. and Papanikolopoulos (1996). Vision-guided robotic grasping: Issues and experiments. In *ICRA'96*, pages 3203–3208.

Tsai, R. Y. and Lenz, R. K. (1989). A new techniques for fully autonomous and effecient 3d robot hand/eye calibration. *IEEE Trans. on Robotics and Automation*, 5(3):345–358.

Yoshimi, B. H. and Allen, P. K. (1994). Visual control of grasping and manipulation tasks. In *Proc. IEEE International Conf. on Multisensor Fusion and Integration for Intelligent Systems*, pages 575–582, Las Vegas, USA.